enhancement and formation of extended defects, were eliminated.

The new additional F ion implantation technique reduced the diffusion enhancement of As and P at low temperatures and formation of extrinsic defects in n-type silicon.

Acknowledgments

The author is grateful to Dr. S. Ushio (Shin-Etsu Handotai Company, Limited) and R. Muto (now Mrs. R. Takenaka, Seiko Epson Corporation) for support with the XTEM analyses, and M. Yakushiji (Seiko Instruments, Incorporated) and T. Oguchi (Seiko Epson Corporation) for SIMS measurement. Thanks are also due to M. Loader (Seikoi Epson Corporation) for the critical reading of the manuscript.

Manuscript submitted July 24, 1989; revised manuscript received about *ca.* Dec. 12, 1989.

Seiko-Epson Corporation assisted in meeting the publication costs of this article.

REFERENCES

1. S. Iwamatsu and J. Kato, *J. Vac. Soc. Jpn.*, **25,** 735 (1982); J. Kato and S. Iwamatsu, *This Journal,* **131,** 1145 (1984).
2. G. J. Van Gurp, J. W. Slotboom, F. J. B. Smolders, W. T. Stacy, and Y. Tamminga, *ibid.*, **127,** 1813 (1980).
3. R. B. Fair, "Impurity Doping," F. F. Y. Wang, Editor, p. 343, North-Holland Pub. Co., Amsterdam (1981).
4. T. E. Seidel, D. J. Lischner, C. S. Pai, R. V. Knoell, D. M. Maher, and D. C. Jacobson, *Nucl. Instr. Methods,* **B7/8,** 251 (1985).
5. N. R. Wu, D. K. Sadana, and J. Washburn, *Appl. Phys. Lett.*, **44,** 782 (1984).
6. N. Z. Muhammd, Z. H. Lu, W. K. Chu, D. Fathy, and J. J. Wortman, *Mater. Res. Soc. Symp. Proc.*, **52,** 31 (1986).
7. A. Kamger and F. A. Baiocchi, *ibid.*, **52,** 23 (1986).
8. J. C. C. Tsai, D. G. Schimmel, R. B. Fair, and M. Maszara, *This Journal,* **134,** 1508 (1987).
9. H. Strunk, U. Gosele, and B. O. Kolbesen, *Appl. Phys. Lett.*, **34,** 530 (1979).
10. R. M. Harris and D. A. Antoniadis, *ibid.*, **43,** 937 (1983).
11. P. Fahey, R. W. Dutton, and S. W. Hu, *ibid.*, **44,** 777 (1984).
12. K. Nishi and D. A. Antoniadis, *J. Appl. Phys.*, **56,** 3428 (1984).
13. K. Nishi and D. A. Antoniadis, *ibid.*, **59,** 1117 (1985).
14. S. Y. Shiryaev, A. N. Larsen, E. S. Sorensen, and P. T. Petersson, *Nucl. Instr. Methods,* **B19/20,** 507 (1987).
15. R. B. Fair and J. C. C. Tsai, *This Journal,* **124,** 1107 (1977).
16. J. C. C. Tsai, D. J. Schimmel, R. E. Ahrens, and R. B. Fair, *ibid.*, **134,** 2348 (1987).
17. S. J. Pennycook, J. Narayan, and O. W. Holland, *J. Cryst. Growth,* **70,** 597 (1984).
18. S. J. Pennycook, J. Naratan, and O. W. Holland, *This Journal,* **132,** 1962 (1985).
19. R. J. Culbertson and S. J. Pennycook, *Nucl. Instr. Methods.*, **B13,** 490 (1986).
20. S. J. Pennycook and R. J. Culbertson, *Mat. Res. Soc. Symp. Proc.*, **52,** 37 (1986).
21. A. J. R. de Kock and W. M. Van de Wijgert, *J. Cryst. Growth,* **49,** 718 (1980).
22. S. M. Hu, P. Fahey, and R. W. Dutton, *J. Appl. Phys.*, **54,** 6912 (1983).
23. F. N. Schwettmann and D. L. Kendall, *Appl. Phys. Lett.*, **21,** 2 (1972).
24. D. Wouters, D. Avau, P. Mertens, and H. E. Maes, *Mat. Res. Soc. Symp. Proc.*, **52,** 217 (1986).
25. S. N. Hsu and L. J. Chen, *Appl. Phys. Lett.*, **55,** 2304 (1989).

Reactive Ion Etching of InAs, InSb, and GaSb in CCl_2F_2/O_2 and C_2H_6/H_2

S. J. Pearton, W. S. Hobson, and F. A. Baiocchi

AT&T Bell Laboratories, Murray Hill, New Jersey 07974

K. S. Jones

University of Florida, Gainesville, Florida 32611

ABSTRACT

Reactive ion etching (RIE) of InAs, InSb, and GaSb in either CCl_2F_2/O_2 or C_2H_6/H_2 discharges has been examined as a function of gas composition, flow rate, pressure, power, and etching time. The C_2H_6/H_2 chemistry gives smooth, controlled etching of these materials for C_2H_6 concentrations less than 40% by volume in H_2, and the etch rates are in the range 280-350Å under these conditions. Subsurface lattice disorder was restricted to ≤50Å in depth for both types of etching. The CCl_2F_2/O_2 chemistry led to consistently rougher surface morphologies on all three materials with In droplets visible on InAs. The etch rates with CCl_2F_2/O_2 are higher by factors of 2-5 than for C_2H_6/H_2, and the etched surfaces all show significant concentrations of Cl-containing residues.

There are a number of important applications for InAs, GaSb, and InSb. In particular, thin epitaxial layers of InAs are used to facilitate ohmic contact formation to GaAs because of the low (~0.2 eV) barrier heights for metals on InAs (1, 2). Gallium antimonide is the optimum substrate for some long wavelength lasers and photodetectors (3-5), while InSb has also attracted much interest as a material for long wavelength (5.3 μm) infrared detectors and emitters. All of these semiconductors have relatively narrow bandgaps and have been used in a variety of superlattice structures with novel transport properties (6). In order to fabricate such structures with ultrasmall geometries, it is necessary to develop dry etching techniques which allow highly anisotropic or selective etching of the component layers. To date there has been very little work carried out on reactive ion etching (RIE) of InAs, GaSb, or InSb because of their relative newness in terms of device utilization.

The most common gas chemistry for dry etching of III-V semiconductors has been based on chlorine or chlorine-containing gas mixtures, primarily because of the high volatilities of Ga, As, P, and Sb chlorides (7-14). For some applications however, Cl-based RIE presents problems because the etch rates tend to be rather large for many III-V

materials, and therefore are not controlable for mesa etching where small thicknesses are removed. In addition, the reactive ion etching of In-based materials tends to leave rough surface morphologies because indium chlorides have lower volatilities than their group V counterparts. The use of chloro-fluorocarbons like CCl_2F_2 (Freon 12) reduces the problems associated with the corrosiveness and toxicity of chlorine, although recent environmental concerns appear likely to lead to restrictions on the use of chloro-fluorocarbons because of their deleterious effect on the earth's ozone layer. Some moves have already been made to ban their use.

Recently a new gas chemistry for etching III-V semiconductors has been introduced. It involves the use of methane- or ethane-hydrogen mixtures, and smooth, controlled etching has been demonstrated for InP, GaAs, InGaAs, and InGaAsP (15-20). The etch products with this gas chemistry are AsH_3 or PH_3 when GaAs or InP are the substrates (21), while the group III product has not been unambiguously identified, although metalorganics such as trimethylgallium and trimethylindium have been suggested (22).

In this paper we report an investigation of the etching characteristics of InAs, GaSb, and InSb in both C_2H_6/H_2 and CCl_2F_2/O_2 discharges. The etch rates have been measured as a function of etching time, total pressure, plasma power density, gas composition, and gas flow rate, and the resultant surface morphology examined by scanning electron microscopy (SEM). Near-surface lattice disorder induced by energetic ion bombardment was investigated by cross-sectional transmission electron microscopy (TEM) and He^+ ion channeling. The elemental composition in the top 100Å of the etched samples was obtained from Auger electron spectroscopy (AES) and x-ray photoelectron spectroscopy (XPS) measurements.

Experimental

All of the wafers used in these experiments were cut from nominally undoped, (100) boules grown by the liquid-encapsulated Czochralski (LEC) technique (Sumitomo Electric, New York). The substrates were 1-2 in. diam, with the InAs being n-type with a 300 K carrier concentration of 10^{16} cm^{-3} and mobility of 25,000 $cm^2 \cdot V^{-1} \cdot s^{-1}$. The InSb was intrinsic at room temperature with a net carrier concentration of 1.7×10^{16} cm^{-3} and an electron mobility of 65,000 $cm^2 \cdot V^{-1} \cdot s^{-1}$. Undoped GaSb is always p-type because of the presence of stoichiometry-related residual acceptors (23-25), and in our case the material displayed a 300 K doping density of $p = 1 \cdot 8 \times 10^{17}$ cm^{-3}, with a hole mobility of 740 $cm^2 \cdot V^{-1} \cdot s^{-1}$.

Prior to patterning with photoresist, the substrates were chemically etched in order to remove any residual polishing damage which might affect the dry etch rates. For the InAs this consisted of etching for 3 min in 2% Br_2/methanol, a rinse in methanol, and a 3 min etch in HF, followed by rinsing in distilled water (26). The GaSb and InSb samples were etched for 3 min in a 5:1:1 H_2SO_4:H_2O_2:H_2O solution at 40°C, rinsed with distilled water, dipped in HF, and rinsed again with distilled water (27). For etch rate measurements, the samples were selectively patterned with AZ1350J photoresist to give a mask with openings of size 1-50 μm in width. These mask openings were descummed by exposure to a 50W O_2 plasma in a barrel reactor, and immediately prior to loading in the RIE systems, the samples were rinsed in 1:1 NH_4OH:H_2O to remove native oxide from the semiconductor.

The samples were reactively ion etched in a Model 51 Materials Research Corporation reactor with a stainless steel chamber and lower powered electrode. We found it necessary to use a quartz cover plate over the cathode in order to achieve reproducible etch rates, and the samples were thermally bonded to the cooled electrode with high vacuum grease. The sample temperature was ≤40°C during all runs. The discharge frequency was 13.56 MHz, with an electrode spacing of 7 cm. Electronic mass flow controllers were used to introduce research-grade C_2H_6, H_2, CCl_2F_2, and O_2 into the chamber after pumping it to a base pressure of ~10^{-7} torr. The InAs, GaSb, and InSb etch rates were examined for their dependence on total pressure (3-40 mtorr), plasma power density (0.4-1.3 W · cm^{-2}), gas composition (5-50% for C_2H_6 relative to H_2, and 25-95% for CCl_2F_2 relative to O_2), gas flow rate (5-25 sccm), and etch time (1-12 min).

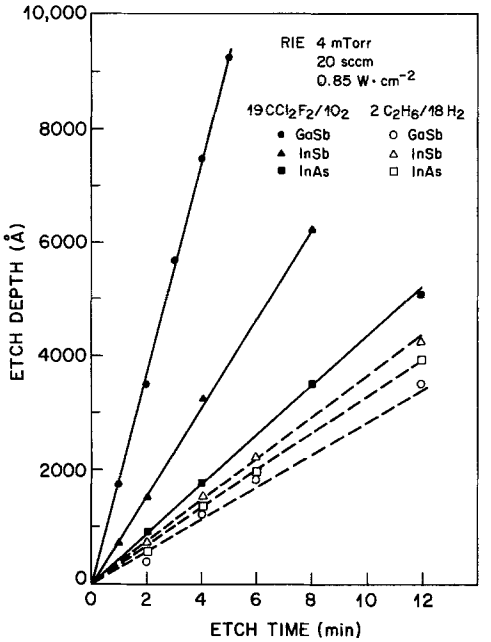

Fig. 1. Etched depth in GaSb, InSb, and InAs as a function of time in discharges of 2 C_2H_6/18 H_2 or 19 CCl_2F_2/1 O_2 (4 mtorr, 0.85 W · cm^{-2}).

After the RIE treatments, the photoresist on patterned samples was removed by rinsing in acetone and methanol, and the etch depth measured by Dektak stylus profilometry on eight spatially separated locations on each 5 × 5 mm^2 sample. The surface morphology was examined by SEM by cleaving through the features on the mask consisting of 1 μm lines separated by 3 μm. A thin Au film (~50Å thick) was deposited on the sample surface to reduce electrical charging, and a primary electron voltage of 20 kV was used. All of the micrographs were taken at 80° with respect to the horizontal. Unpatterned sections were also prepared for cross-sectional TEM by chemical thinning and iodine ion milling. The latter proved to be an absolute necessity in order to reduce ion milling damage in the InAs, GaSb, and InSb. A JEOL 200CX microscope was used, and all micrographs were taken using multibeam

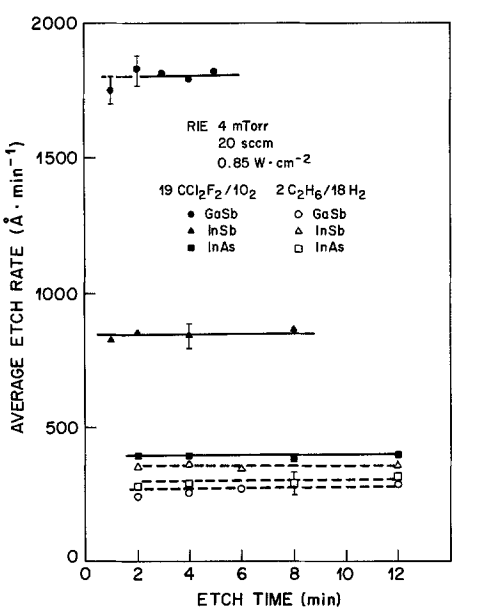

Fig. 2. Average etch rate of GaSb, InSb, and InAs as a function of time under the discharge conditions of Fig. 1.

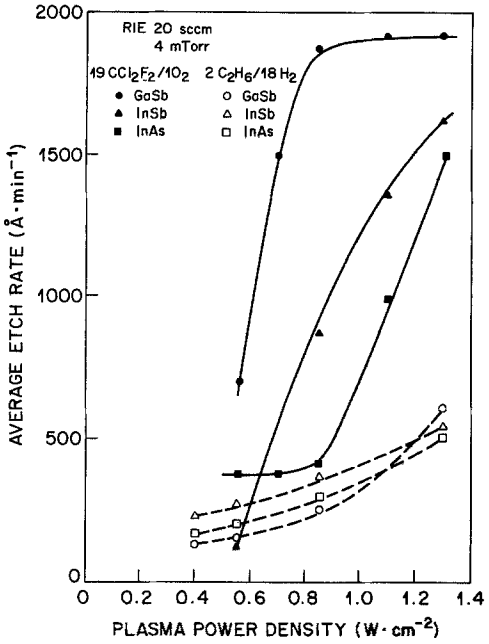

Fig. 3. Average etch rate of GaSb, InSb, and InAs as a function of the plasma power density for 4 mtorr 2 $C_2H_6/18$ H_2 or 19 $CCl_2F_2/1$ O_2 discharges.

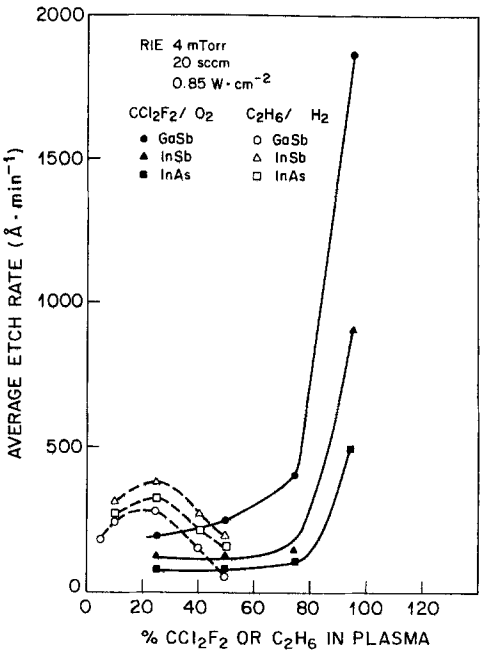

Fig. 5. Average etch rate of GaSb, InSb, or InAs as a function of gas composition in 4 mtorr, 0.85 W · cm^{-2} C_2H_6/H_2 or CCl_2F_2/O_2 discharges.

bright field imaging with seven beams included within the objective aperture. The sample was tilted so that the beam direction was parallel to the [110] zone axis in order to reduce contrast effects at the surface and allow the best view of the surface morphology.

Samples for AES were examined with a primary electron beam voltage of 10 kV at a beam current of 0.5 μA and a primary beam spot size of 5 μm diam. Depth profiling was accomplished by sputtering the sample with 3.5 keV Ar^+ ion beam at a rate of ~40Å · min^{-1}, rastered over 3 × 3 mm^2. XPS with angle-resolved capabilities was used to measure both the atomic composition of the near-surface region and the chemical bonding of the In, Sb, Ga, and As atoms. All chemical analyses were performed after removal from the RIE chamber to give a picture of what the surface will be like in a typical device processing sequence. We also performed the analyses with different beam currents in order to check that the beam itself was not changing the surface chemistry. We found no evidence of any alteration by the probe beam.

Results and Discussion

Etch rate dependencies.—It is clear, from the original work of Niggebrugge *et al.* (15), that reproducible, polymer-free etching, at least for InP, is obtained for small fractions of ethane or methane relative to hydrogen for the C_2H_6/H_2 or CH_4/H_2 gas chemistry. Our own experience with Freon 12 RIE has been that a small addition of O_2 to the discharge minimizes polymeric residues on the etched surfaces (20). Based on these results we chose as our standard etching condition 2 $C_2H_6/18$ H_2 or 19 $CCl_2F_2/1$ O_2 mixtures, each at a total pressure of 4 mtorr, flow rate of 20 sccm, and a power density of 0.85 W · cm^{-2}. The self-biases on the cathode under these conditions were 430V for the C_2H_6/H_2 discharges and 390V for CCl_2F_2/O_2.

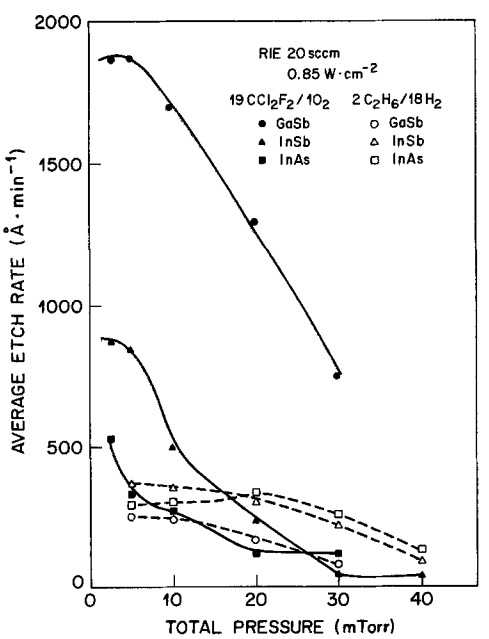

Fig. 4. Average etch rate of GaSb, InSb, and InAs in 0.85 W · cm^{-2} 2 $C_2H_6/18$ H_2 or 19 $CCl_2F_2/1$ O_2 discharges as a function of the total pressure in the reactor.

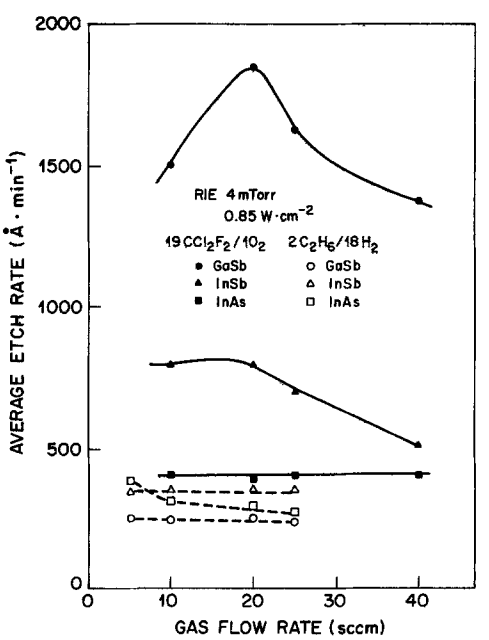

Fig. 6. Average etch rate of GaSb, InSb, or InAs in 4 mtorr, 0.85 W · cm^{-2} 2 $C_2H_6/18$ H_2 or 19 $CCl_2F_2/1$ O_2 discharges, as a function of gas flow rate.

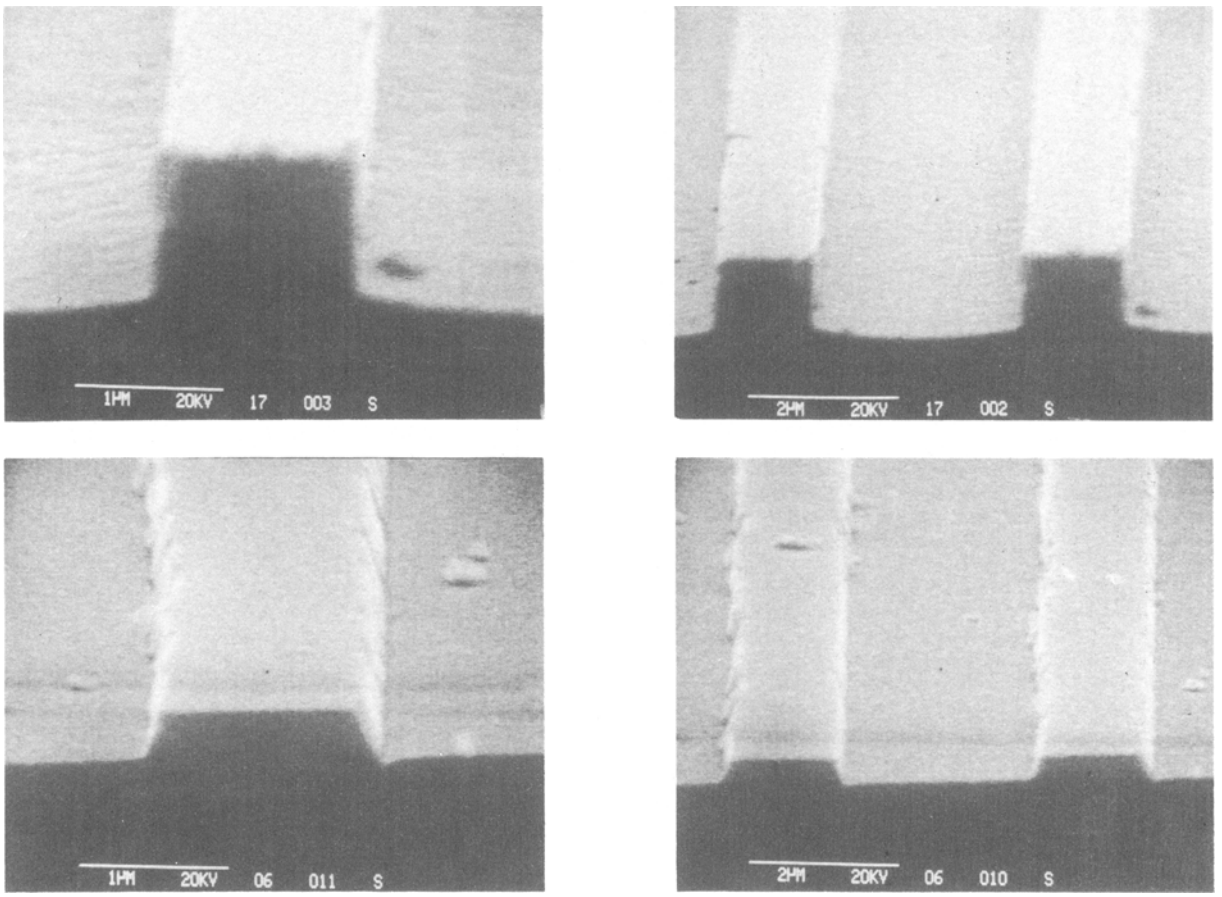

Fig. 7. SEM micrographs from GaSb reactively ion etched in 4 mtorr, 20 sccm, 1.1 W · cm^{-2} discharges of 19 CCl_2F_2/1 O_2 (at top) and 2 C_2H_6/18 H_2 (at bottom) for 4 min each.

Figure 1 shows the time dependence of etch depth in InAs, GaSb, and InSb for RIE times up to 12 min. All of the lines pass through the origin, implying that there is no delay in the commencement of etching upon ignition of the plasma as is often observed for RIE of materials like AlGaAs which have thick native oxides. The etch depths are all linear with time, and in each case the CCl_2F_2/O_2 etching is faster than for comparable treatments with C_2H_6/H_2. It appears from these results that gallium and antimony chlorides are more volatile under RIE conditions than their indium and arsenic counterparts. The normal boiling points of these possible etch products are $GaCl_3$ (201°C), $GaCl_2$ (535°C), $SbCl_3$ (283°C), $SbCl_5$ (79°C), $AsCl_3$ (130°C), InCl (608°C), $InCl_2$ (560°C), and $InCl_3$ (600°C) (8), although these should be used as a guide only in considering etch rates since it is their volatility under ion bombardment that is the critical parameter. The vapor pressure at 75°C of $AsCl_3$ is 19 torr and of $GaCl_3$ is 14.5 torr, to give some idea of their relative volatility (29, 30). By contrast to the results for CCl_2F_2/O_2 RIE, the use of C_2H_6/H_2 leads to the slowest etch rates for GaSb which is consistent with past reports of decreasing etch rates for increasing Ga content in the material (15). The average etch rates of InAs, InSb, and GaSb as a function of etch time are shown in Fig. 2. Within experimental error these etch rates show no time dependence.

Figure 3 shows the dependence on plasma power density of the etch rates of InAs, InSb, and GaSb in C_2H_6/H_2 or CCl_2F_2/O_2. The results for C_2H_6/H_2 RIE are all fairly similar, showing monotonic increases in etch rate as the power density, and hence self-bias (V_B) on the cathode, increased. The ion current incident on the sample will also increase under these conditions as it is proportional to $V_B^{3/2}$. For this gas mixture the self-bias was 200V at 0.4 W · cm^{-2} and 610V at 1.3 W · cm^{-2}, leading to more efficient sputter-induced desorption of the etch products at the higher powers. The results for CCl_2F_2/O_2 RIE of these materials are quite different from each other. For GaSb there is a saturation in etch rate for power densities above ~0.8 W · cm^{-2}, indicating that the reactive species from the discharge may be removed by ion bombardment before they have a chance to react with the semiconductor. By contrast, InSb does not show this behavior, although it is possible that it occurs at power densities higher than those we investigated. Finally, for InAs the etch rate is constant up to ~0.8 W · cm^{-2} at which point it increases rapidly with increasing power density. This would be consistent with a desorption-limited etch regime at the lower power densities.

The etch rate dependence on the total pressure in the reactor at constant flow rate (20 sccm) and plasma power density (0.85 W · cm^{-2}) is shown in Fig. 4. The GaSb, InSb, and InAs etched in C_2H_6/H_2 all show a decrease in etch rate with increasing pressure, which is presumably due to the decrease in cathode self-bias (430V at 4 mtorr, 225V at 30 mtorr). Even though the fall-off in etch rate appears to be even more dramatic for CCl_2F_2/O_2 RIE with increasing pressure, the proportionate decreases are of the same order as for C_2H_6/H_2 etching factors of approximately 3-5 over the pressure range 4-40 mtorr for both gas chemistries. Therefore, we appear to be in a desorption-limited regime under these conditions, because in a reactant-limited mode the etch rate should increase as the pressure and hence number of reactive species supplied to the surface increases.

The effect of altering the gas composition of the two different types of discharge on the etch rates of GaSb, InSb, and InAs is shown in the data of Fig. 5. For the C_2H_6/H_2 chemistry the etch rates for all three materials peak around 25% of C_2H_6 by volume in the plasma. This is consistent with results on RIE of InP and GaAs using C_2H_6/H_2 or CH_4/H_2, in which maximum etch rates are observed at 10-20% by volume of the organic component (15, 17, 19). The increase in etch rate we observe for C_2H_6 fractions up to 0.25 is presumably due to an increase in the concentration of active species like ethyl radials, while above 25% C_2H_6 by volume there is most likely a competition between

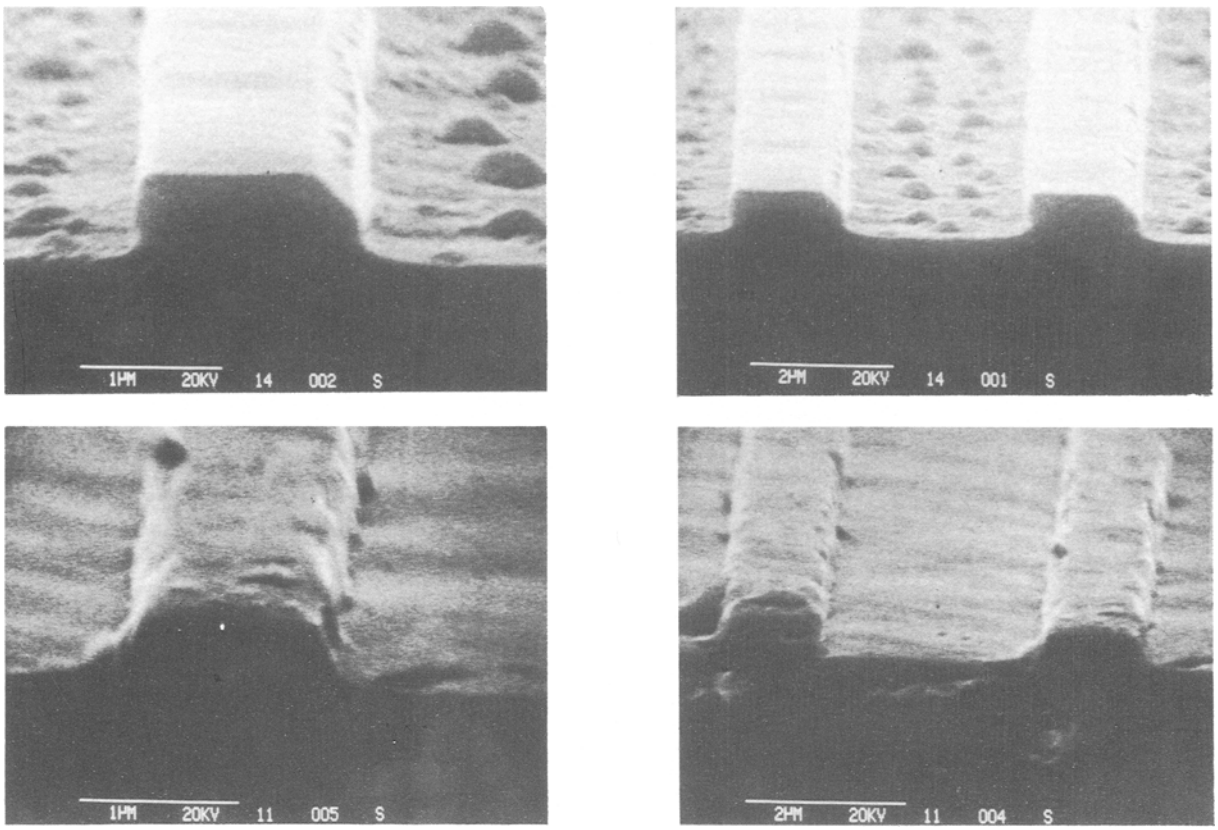

Fig. 8. SEM micrographs from InAs reactively ion etched in 4 mtorr, 20 sccm, 1.1 W · cm^{-2} discharges of 19 CCl_2F_2/1 O_2 (at top) or 2 C_2H_6/18 H_2 (at bottom) for 4 min each.

etching and polymer deposition, with a consequent decrease in etch rate. At C_2H_6 concentrations above 40% we observed a brown film on the photoresist mask and heavy polymer deposition around the reactor chamber. By contrast, GaSb, InSb, and InAs reactively ion etched in CCl_2F_2/O_2 show little change in etch rate until a concentra-

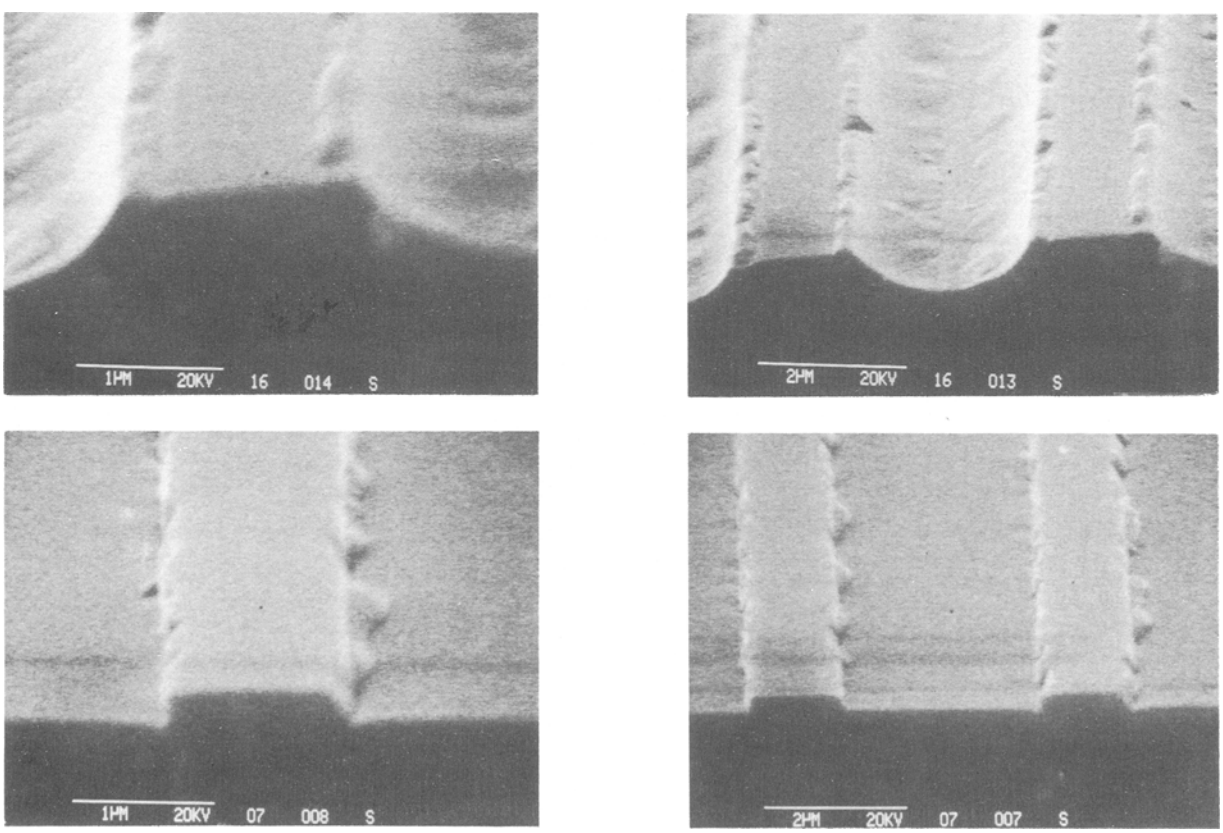

Fig. 9. SEM micrographs of InSb reactively ion etched in 4 mtorr, 20 sccm, 1.1 W · cm^{-2} discharge of 19 CCl_2F_2/1 O_2 (at top) or 2 C_2H_6/18 H_2 (at bottom) for 4 min each.

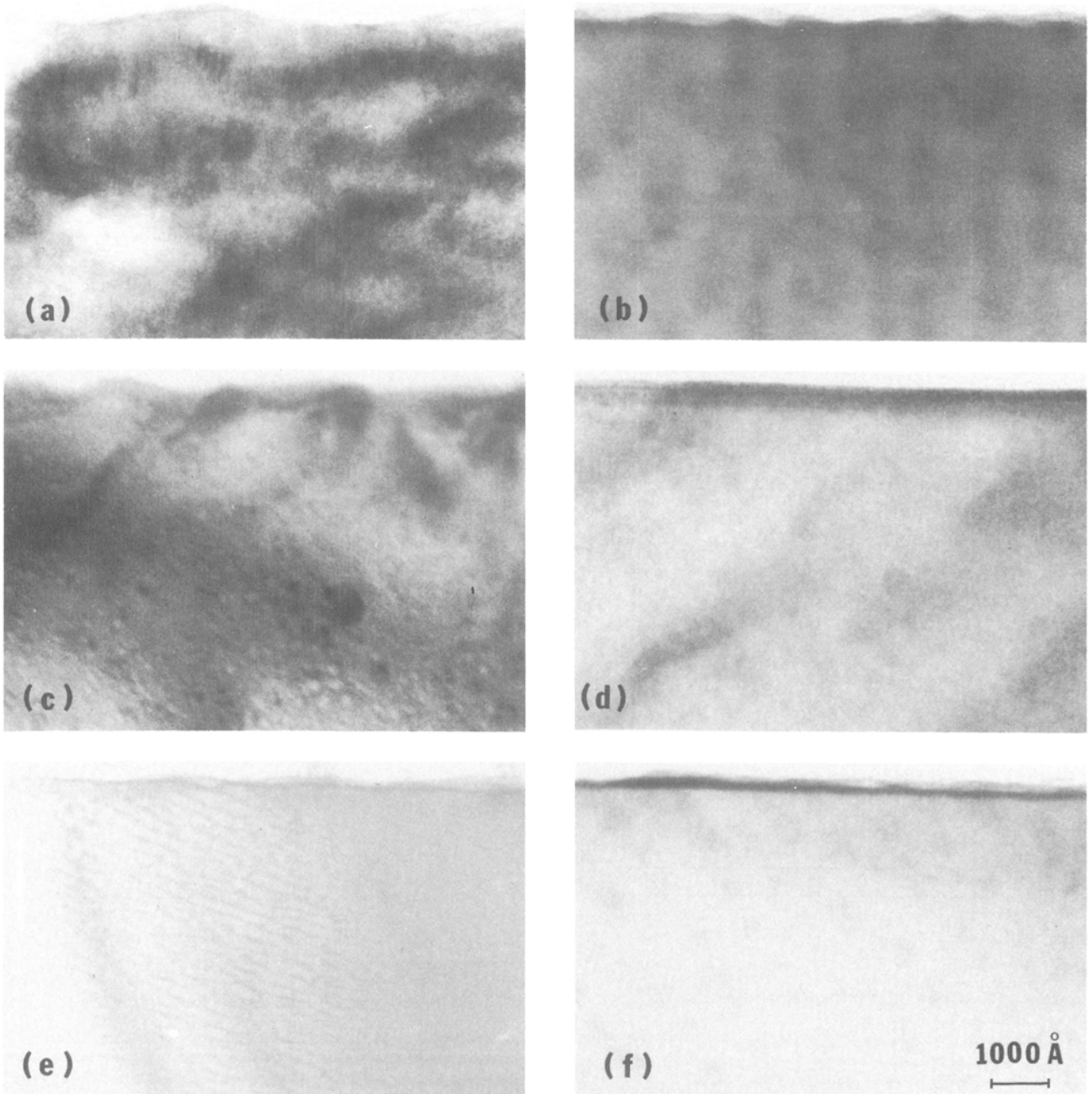

Fig. 10. TEM cross sections from GaSb etched in (a) 19 CCl_2F_2/1 O_2 or (b) 2 C_2H_6/18 H_2; InSb etched in (c) 19 CCl_2F_2/1 O_2 or (d) 2 C_2H_6/18 H_2; and InAs etched in (e) 19 CCl_2F_2/1 O_2 or (f) 2 C_2H_6/18 H_2 discharges, each for 4 min under the conditions of Fig. 9.

tion of 75% by volume of Freon 12, at which point this rate increases sharply. This rapid increase is also presumably due to an increase in the concentration of active chlorine species available for reaction at the semiconductor surface. The largest differential in etch rate between the two gas chemistries is obtained with GaSb.

Under our conditions, the etch rates of all three materials are independent of the gas flow rates for C_2H_6/H_2 RIE, as shown in Fig. 6. The nominal residence times in our reactor vary from 1.25-0.16s for flow rates between 5-40 sccm, but these times appear to be longer than the surface reaction time for removal of Ga, Sb, In, and As during C_2H_6/H_2 RIE. The results for CCl_2F_2/O_2 etching are quite different, with InAs showing no flow rate dependence, InSb displaying a decrease in etch rate with increasing flow rate, and GaSb actually going through a maximum with increasing flow rate. This could be explained as follows: up to a flow rate of 20 sccm there is an increase in the number of active chlorine species per unit time reaching the surface of the semiconductor, leading to an increase in etch rate. Above 20 sccm these active species are pumped away before they can react with the GaSb. We did not observe any change in deposition within the reactor with increasing gas flow, so the alternative explanation of having deposition up to 20 sccm, beyond which the products are pumped away more efficiently, does not seem likely.

Surface morphology and damage.—For GaSb we obtained smooth surface morphologies after etching with either gas chemistry over a wide range of discharge conditions. Figure 7 shows SEM micrographs from GaSb samples reactively ion etched under similar conditions (4 mtorr, 4 min, 20 sccm, 1.1 $W \cdot cm^{-2}$) in either a 19 CCl_2F_2/1 O_2 (at top) or a 2 C_2H_6/18 H_2 (at bottom) plasma. The etch rate is faster for the former leading to a deeper mesa, but in both cases the etched surface is featureless. The anisotropy of the etching appears a little better for CCl_2F_2/O_2 RIE, and the sidewall for features etched in C_2H_6/H_2 shows some waviness. We have observed similar results for etching of GaAs and InP in C_2H_6/H_2. At this point it is not clear what causes the waviness because we have seen no evidence for polymer deposition on the sidewall. Under our

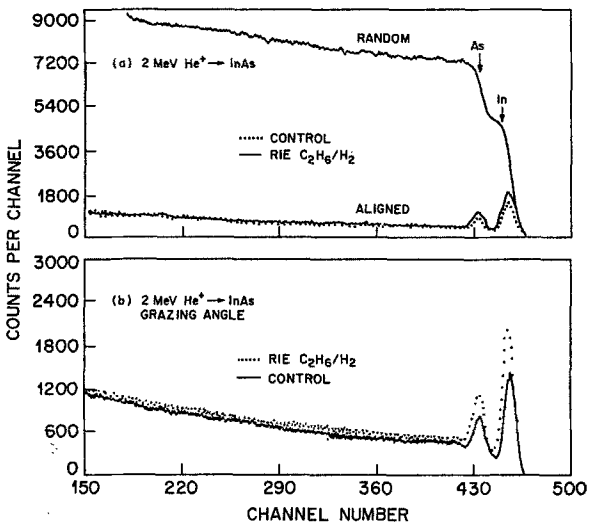

Fig. 11. Ion channeling spectra taken in (a) conventional or (b) grazing angle geometries using 2 MeV He^+ ions on InAs control or RIE (1.1 W · cm^{-2}, 4 mtorr, 4 min, 20 sccm) samples.

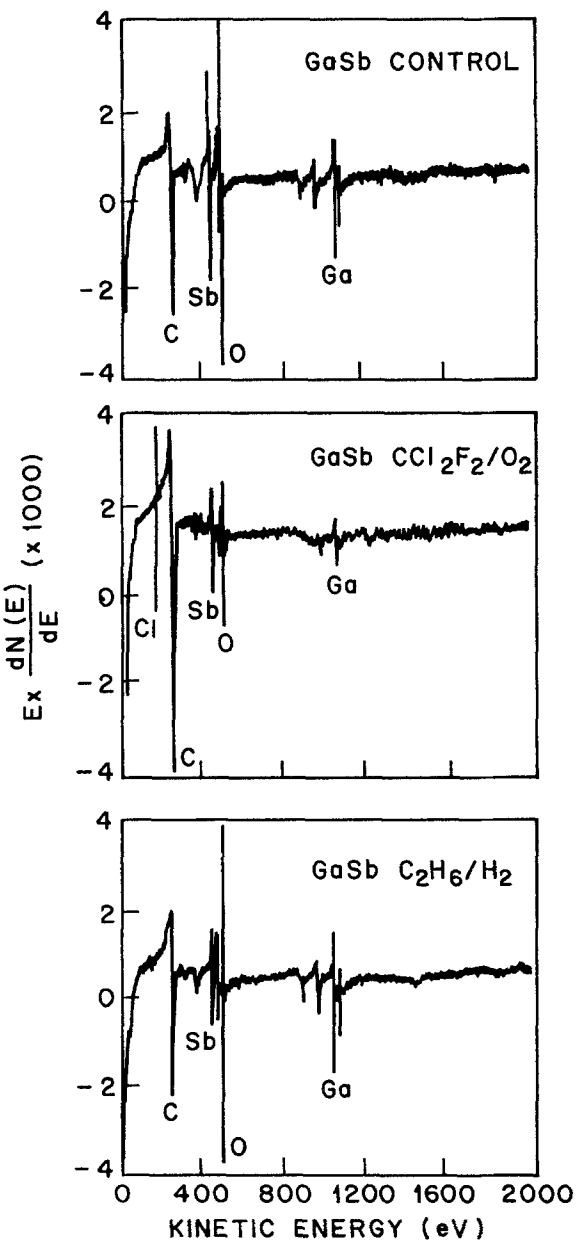

Fig. 12. AES survey spectra from control or RIE GaSb samples (4 min, 4 mtorr, 0.85 W · cm^{-2}, 2 C_2H_6/18 H_2 or 19 CCl_2F_2/1 O_2 discharges).

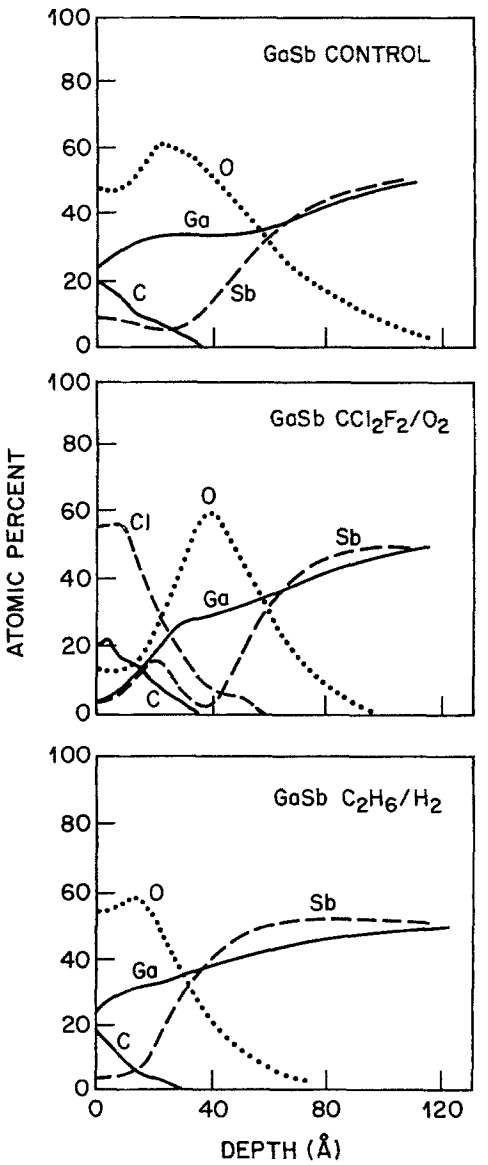

Fig. 13. AES depth profiles of elemental composition in the near-surface region of GaSb control or RIE samples (conditions of Fig. 12).

conditions smooth etching of the wafer surface itself was obtained for all C_2H_6 concentrations less than 40% by volume in the discharge. For C_2H_6 fractions above this value, there was increasing undercutting of the sidewalls and

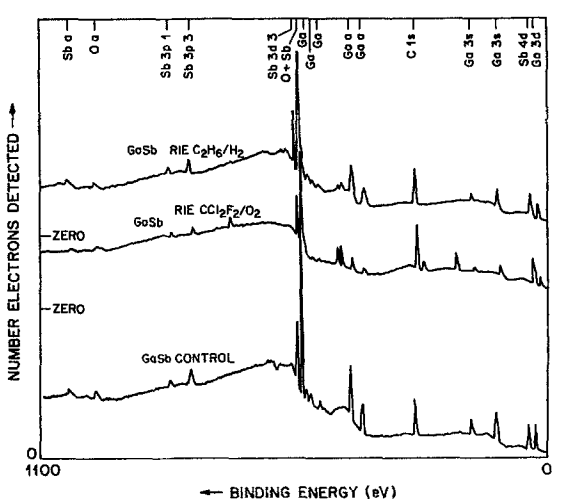

Fig. 14. XPS survey spectra from GaSb control or RIE samples (conditions of Fig. 12).

Table I. XPS results. Elemental composition data measured from the surface (~100Å) of each sample and expressed in atomic percent units for the elements detected

Sample	C	O	F	Cl	Ga	As	In	Sb
InAs-control	40	34	—	—	—	10	16	—
InAs-C_2H_6/H_2	32	39	—	—	—	11	18	—
InAs-CCl_2F_2/O_2	48	27	—	7.5	—	9	8.5	—
InSb-control	32	44	—	—	—	—	12	12
InSb-C_2H_6/H_2	36	38	—	—	—	—	14	11
InSb-CCl_2F_2/O_2	28	45	—	4.2	—	—	7.9	14.9
GaSb-control	40	39	—	—	13	—	—	8.2
GaSb-C_2H_6/H_2	30	44	—	—	18	—	—	7.8
GaSb-CCl_2F_2/O_2	44	33	2.8	6.3	5.4	—	—	8.5

RIE conditions: 2 C_2H_6/18 H_2, 0.85 W · cm^{-2}, 4 mtorr; 19 CCl_2F_2/1 O_2, 0.85 W · cm^{-2}.

very rough surface morphologies. We attribute a large part of this roughness to sputtering of polymer from on top of the photoresist mask onto the horizontal surface. This leads to a micromasking effect on this surface, with the consequent roughening of the morphology.

The surfaces on InAs reactively ion etched in both types of discharge were not as smooth as with GaSb. Figure 8 shows SEM micrographs from InAs samples etched in CCl_2F_2/O_2 (top) or C_2H_6/H_2 (bottom) under the same conditions described earlier. For CCl_2F_2/O_2 RIE there are In droplets visible on the etched surface, which implies a severe As deficiency for these discharge conditions. This kind of surface degradation is usually observed after exposure of InP and related compounds to hydrogen-based plasmas (31) but can often be seen with Cl_2-based RIE of InP as well. The etching of InAs in C_2H_6/H_2 does not lead to In droplet formulation, but the surface morphology is not particularly good. At least part of this seems to have been caused by the wet etching treatment prior to the photoresist being spun-on. The evidence for this assertion comes from the fact that the surface of the areas that were masked during RIE are also quite wavy, meaning that most of the surface features observed on the mesa bottom were not in fact a result of the dry etch.

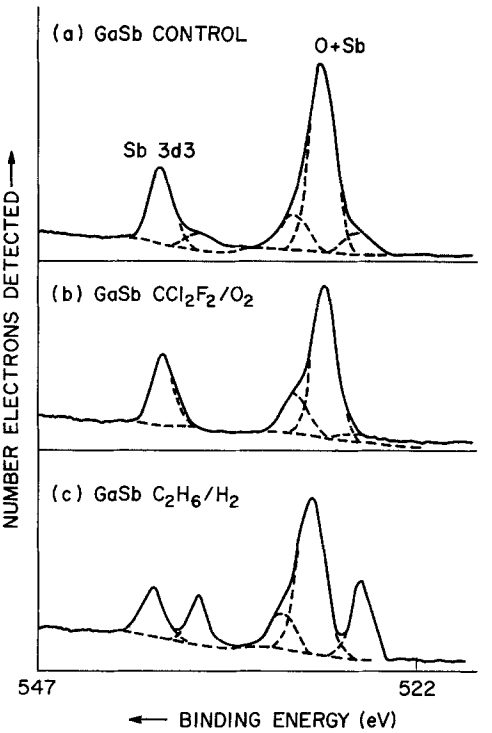

Fig. 15. High-resolution XPS Sb(3d3) and Sb+O data from GaSb control or RIE samples (conditions of Fig. 12).

Figure 9 shows SEM micrographs from InSb samples reactively ion etched in CCl_2F_2/O_2 (at top) and C_2H_6/H_2 (at bottom). The discharge conditions were the same as described earlier with regard to Fig. 7 and 8. In the case of CCl_2F_2/O_2 RIE, severe overcutting of the mesa is obvious and there is a good deal of roughness apparent in the field of view of the SEM. The overcutting may be due to involatile etch products sticking to (and masking) the sidewalls.

Table II. High-resolution ESCA data: binding energies, atom percentages, and peak assignments. (Binding energies were corrected to the binding energy of the —CH_2CH_2— signal at 284.6 eV. Atom percentages were calculated from the high-resolution data. Peak assignments were based on the binding energies of the reference compounds.)

Sample	C_1	C_2	C_3	O_1	O_2	Ga_1	Ga_2	As_1	As_2	As_3	Sb_1	Sb_2	In_1	In_2	Cl_1	Cl_2
InSb control																
Binding energies	284.6	286.1	288.3	—	—	—	—	—	—	—	536.9	539.5	—	444.5	—	—
Atom percents	21.	6.3	5.0	—	—	—	—	—	—	—	2.3	8.7	—	14.	—	—
InSb C_2H_6/H_2																
Binding energies	284.6	286.0	288.5	—	—	—	—	—	—	—	536.9	539.5	—	444.5	—	—
Atom percents	27.	5.3	3.9	—	—	—	—	—	—	—	2.4	8.6	—	14.	—	—
InSb CCl_2F_2/O_2																
Binding energies	284.6	286.3	288.7	—	—	—	—	—	—	—	537.7	539.8	—	445.0	198.4	—
Atom percents	22.	2.1	1.5	—	—	—	—	—	—	—	1.0	13.	—	7.9	4.6	—
InAs control																
Binding energies	284.6	286.1	288.1	530.8	532.3	—	—	40.5	43.7	45.0	—	—	443.9	444.9	—	—
Atom percents	28.	6.7	4.8	25.	8.9	—	—	6.3	1.8	1.9	—	—	9.6	6.4	—	—
InAs C_2H_6/H_2																
Binding energies	284.6	286.1	288.2	530.8	532.2	—	—	40.7	43.7	45.0	—	—	444.0	445.0	—	—
Atom percents	25.	3.2	3.2	29	10.	—	—	6.5	2.5	2.1	—	—	10.	7.5	—	—
InAs CCl_2F_2/O_2																
Binding energies	284.6	286.1	288.5	531.1	532.4	—	—	41.3	43.7	45.2	—	—	—	445.2	198.5	—
Atom percents	34.	9.3	4.7	18.	5.7	—	—	1.6	5.0	2.5	—	—	—	8.6	7.3	—
GaSb control																
Binding energies	284.6	286.3	288.3	—	—	19.2	20.2	—	—	—	537.6	539.7	—	—	—	—
Atom percents	31.	3.5	2.5	—	—	3.7	9.3	—	—	—	1.8	6.7	—	—	—	—
GaSb C_2H_6/H_2																
Binding energies	284.6	286.3	288.4	—	—	18.6	20.0	—	—	—	536.9	539.6	—	—	—	—
Atom percents	30.	4.3	2.8	—	—	5.8	12.	—	—	—	3.5	4.3	—	—	—	—
GaSb CCl_2F_2/O_2																
Binding energies	284.6	286.2	288.0	—	—	18.8	20.5	—	—	—	539.0	540.1	—	—	198.8	200.4
Atom percents	31.	9.5	4.0	—	—	1.8	3.6	—	—	—	0.9	6.4	—	—	3.9	2.4

Peak assignments:
C_1 = C—R (R = C, H)
C_2 = C—O—R
C_3 = O=C—O—R
O_1 = metal oxides
O_2 = C=O, C—O—R
In_1 = In, InSb
In_2 = InO_x
Ga_1 = Ga, GaSb
Ga_2 = GaO_x
Sb_1 = Sb, SbIn
Sb_2 = SbO_x
As_1 = As, AsIn
As_2 = As_2O_3
As_3 = As_2O_5
Cl_1 = Cl
Cl_2 = C—Cl

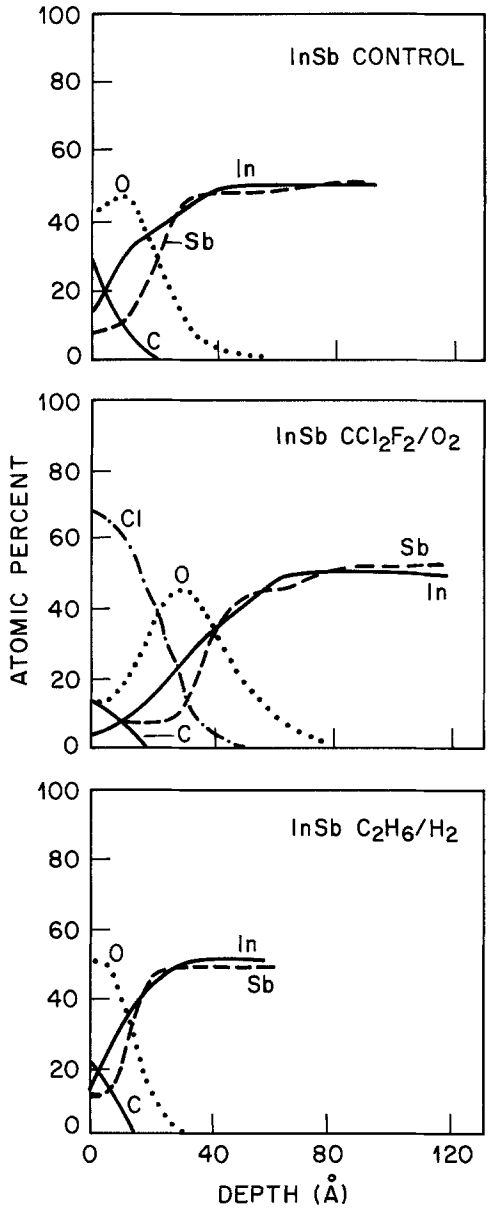

Fig. 16. AES survey spectra from InSb, control or RIE samples (4 min, 0.85 W · cm^{-2}, 4 mtorr, 2 C_2H_6/18 H_2 or 19 CCl_2F_2/1 O_2 discharges).

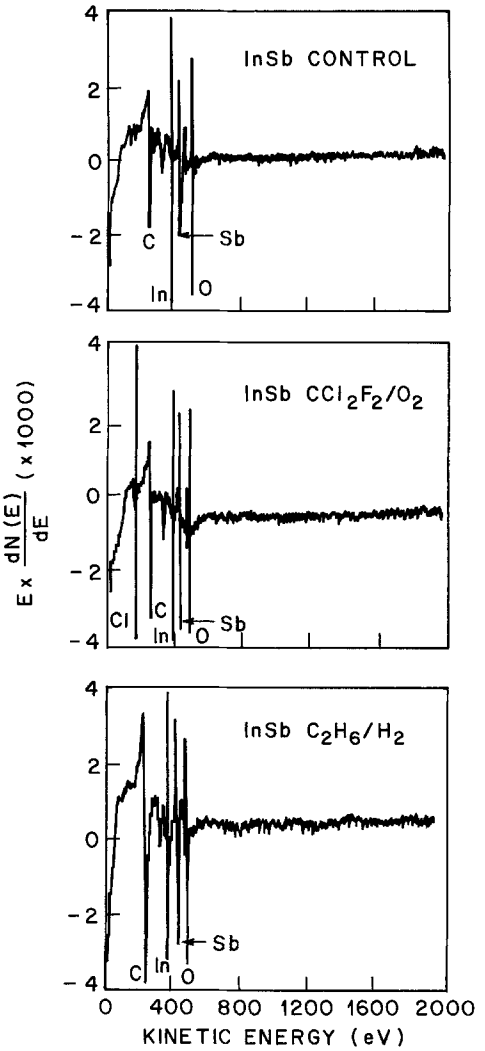

Fig. 17. AES depth profiles of elemental composition in the near-surface region of InSb control or RIE samples (conditions of Fig. 16).

By contrast, C_2H_6/H_2 RIE leads to featureless surface morphologies, but rather rough sidewalls. We did not observe any correlation between the roughness of the sidewalls and more severe undercuttinig. The origin of the sidewall roughness is not clear, although it may be due to replication of edge roughness in the mask. In almost all cases we observed a faithful transfer of the mask dimensions into the sample, with no significant loss of feature size. In general it appears that CCl_2F_2/O_2 etching leads to somewhat rougher morphologies than for RIE with C_2H_6/H_2, at least for the materials discussed here.

This conclusion is supported by the cross-sectional TEM micrographs of Fig. 10. On the left-hand side of the figure we show micrographs from GaSb, InSb, and InAs reactively ion etched in CCl_2F_2/O_2 under the same conditions described previously for the SEM pictures, while on the right-hand side of the figure we show the corresponding micrographs from C_2H_6/H_2-etched samples. In each case the latter samples have comparable or better surface morphologies. For the CCl_2F_2/O_2 etching, the GaSb showed peak-to-valley roughness of 100-120Å, the InSb had peak-to-valley heights of 120-150Å, and finally InAs had values of 80-90Å. By contrast, the peak-to-valley roughness of these materials after C_2H_6/H_2 RIE were GaSb (50-60Å), InSb (<20Å), and InAs (<30Å). Even under these high power density (1.1 W · cm^{-2}) conditions there were no subsurface dislocations observed after RIE, as we have seen with GaAs.

The fact that GaSb, InSb, and InAs are more resistent to the introduction of lattice disorder than GaAs is borne out by ion channeling data from the RIE samples. Figure 11 shows backscattering spectra obtained using 2 MeV He^+ ions at either conventional or glancing angle geometries on reactively ion etched InAs. In the lower part of the figure the width of the In and As surface peaks is ~50Å, which is basically the resolution of the technique given that there will always be a few monolayers of disorder associated with surface reconstruction and the presence of native oxides. After RIE the area under the surface peaks increases, but the width (at half-maximum) remains the same as that of the control sample, indicating that any damage introduced by the C_2H_6/H_2 treatment is limited to a depth of <50Å. It has been our experience that C_2H_6/H_2 discharges operated at similar power densities to CCl_2F_2/O_2 plasmas will create damage at greater depths than the Freon-12 based mixture, because of the greater penetration depth of the light hydrogen ions relative to the ions in this mixture. In GaSb, InSb, and InAs we therefore expect that CCl_2F_2/O_2, even at relatively high plasma power densities, will not lead to the introduction of measurable lattice disorder beyond 50Å.

Surface chemistry.—After RIE the samples were removed from the plasma reactor, and the composition and chemical bonding in the near-surface region were examined by AES and small-area XPS in separate systems. As mentioned earlier, we did not see any effects of the probe beams due to preferential desorption or other changes due to local heating. Although AES and XPS are not sensitive

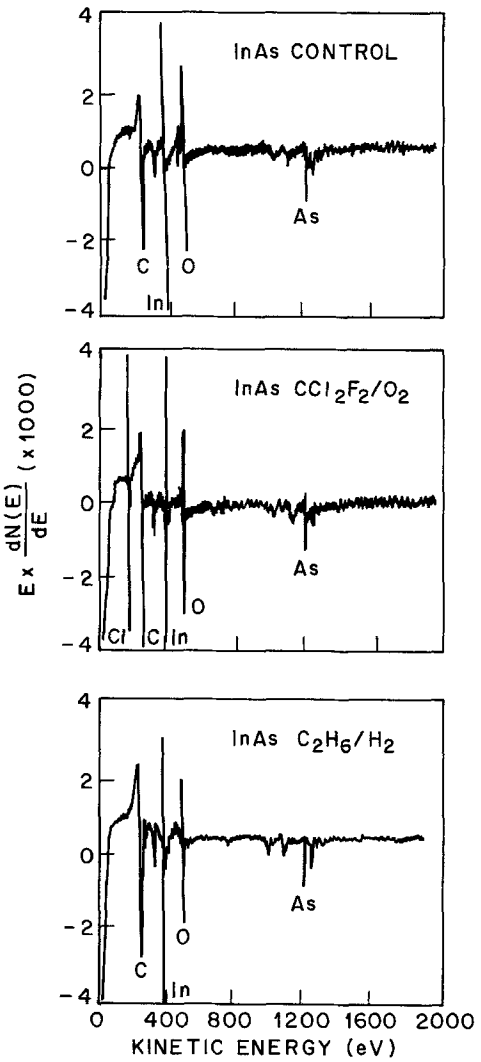

Fig. 18. AES survey spectra from InAs control or RIE samples (4 min, 0.85 W · cm^{-2}, 2 C_2H_6/18 H_2 or 19 CCl_2F_2/1 O_2 discharges).

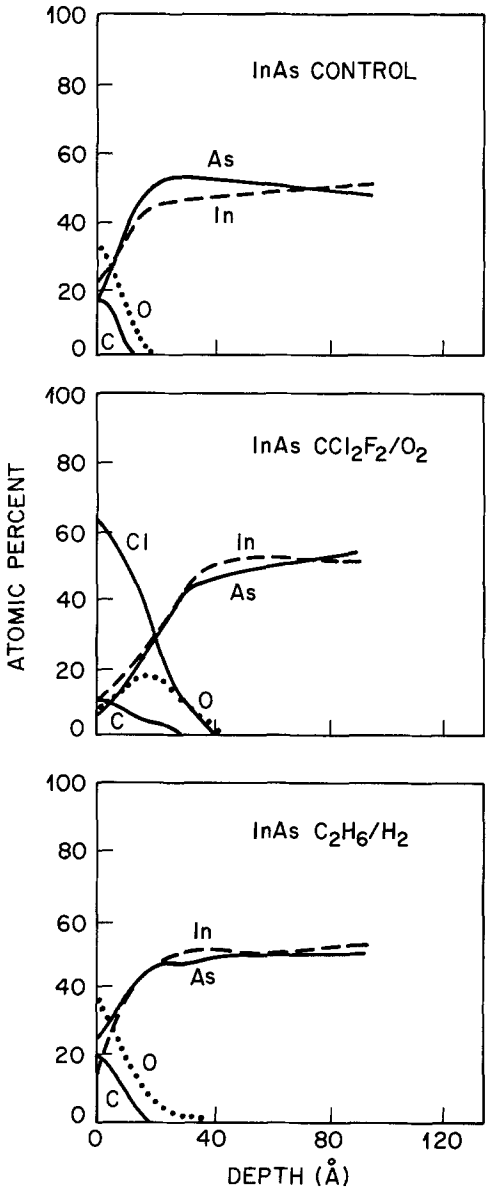

Fig. 19. AES depth profiles of elemental composition in the near-surface region of InAs control or RIE samples (conditions of Fig. 18).

to the presence of hydrogen, we expect that some hydrogen will enter the samples during RIE in C_2H_6/H_2, as it does in GaAs and InP. To this point, however, there has been no demonstration of the role of hydrogen in InAs, InSb, or GaSb, so it is not clear whether passivation of the shallow dopants occurs in these materials. Figure 12 shows AES surface scans of Ga, Sb, O, C, and Cl on GaSb samples etched in either CCl_2F_2/O_2 or C_2H_6/H_2 discharges, as well as results from an unetched control sample. There are two features obvious from this data. First, for CCl_2F_2/O_2 RIE, there is considerable Cl contamination on the surface. Second, etching in the C_2H_6/H_2 discharge leads to an Sb deficiency on the surface. Atomic depth profiles of the composition in the near-surface region are shown in Fig. 13. On the control sample the native oxide appears to be composed predominantly of a gallium oxide. After CCl_2F_2/O_2 RIE, more than 50% of the surface is covered in a Cl species on top of an oxide on the GaSb, whereas after C_2H_6/H_2 RIE, the surface looks chemically very similar to that of the control sample. Any Sb deficiency appears to be less than 40Å in depth in the material etched in the C_2H_6/H_2 discharge.

Figure 14 shows XPS survey spectra from GaSb samples etched in the two different gas chemistries, as well as from an unetched control sample. High-resolution data from these spectra were curve-fitted to resolve the presence of multiple components, and based on this type of data the average elemental composition in the top 100Å of each sample was estimated and is reported in Table I. The surface C concentration varied between 30 and 44 atom percent (a/o), which is within the range expected from atmospheric contamination. Because of the presence of Cl, and a small amount of F, contamination on the surface of the material etched in CCl_2F_2/O_2, it appears to be Ga-poor, but this is an artifact as seen from the AES depth profiles in Fig. 13. The C_2H_6/H_2 gas chemistry appears to be inherently cleaner compared to CCl_2F_2/O_2.

Examples of high-resolution XPS data for Sb(3d3) and O+Sb transitions from control and RIE GaSb samples are shown in Fig. 15. Differences in the relative amounts of the various oxides are obvious, particularly for the C_2H_6/H_2 etched material. The oxygen is present both as metal oxides and C=O and C—O—C or C—O—H species. The tabulation of the high-resolution XPS data giving the binding energies of the different transitions observed, their probable assignments, and atom percent compositions, is listed in Table II. The Ga and Sb are present as both elemental species in the GaSb, and as oxides, and similar results are obtained for the components in the InAs and InSb. It is noticeable that Cl contamination is present on all samples after CCl_2F_2/O_2 RIE, whereas the samples etched in C_2H_6/H_2 appear to be relatively free of surface residues.

AES survey spectra from both etched and unetched InSb samples are shown in Fig. 16. Once again the most obvious point arising from this data is that CCl_2F_2/O_2 RIE leads to the presence of Cl contamination on the surface. This residue is ~40Å thick, as seen in the AES depth profiles of Fig. 17. In this case the Cl residues appear to be present at an even higher concentration than was the case

with GaSb. The sample etched in C_2H_6/H_2 has a surface chemistry very similar to that of the control piece.

Similar data was obtained from InAs samples. Figure 18 shows the AES survey spectra from control and RIE samples for both kinds of gas chemistry. Once again C_2H_6/H_2 RIE leaves a surface of similar composition to that of the control sample, while CCl_2F_2/O_2 RIE leaves a Cl-containing residue. The depth profiles of the elemental composition are shown in Fig. 19, where the Cl is shown to persist to a depth of 40Å after CCl_2F_2/O_2 etching, and there is a deficiency of As to a depth of ~60Å after both C_2H_6/H_2 and CCl_2F_2/O_2 RIE.

Conclusions and Summary

The C_2H_6/H_2 mixture appears to give smooth, controlled etching of GaSb, InSb, and InAs under conditions in which the C_2H_6 fraction by volume is ≤0.4 of the total amount of gas in the mixture. The etch rates for these materials are in the range 280-350Å under our standard conditions (2 C_2H_6/18 H_2, 4 mtorr, 0.85 $W \cdot cm^{-2}$) which is useful for mesa etching applications where only small etch depths are required. The surfaces after C_2H_6/H_2 RIE are residue-free, although for InAs etched at very high power densities, In droplets could be observed due to preferential removal of As. Subsurface lattice disorder is restricted to depths ≤50Å in InAs.

By contrast the CCl_2F_2/O_2 mixture leads to higher etch rates (400 $Å \cdot min^{-1}$ for InAs to ~1800 $Å \cdot min^{-1}$ for GaSb) under our standard conditions (19:1 CCl_2F_2:O_2, 0.85 $W \cdot cm^{-2}$, 4 mtorr) than for C_2H_6/H_2. These etch rates also rise much more rapidly with increasing plasma power density, and on InAs there is preferential removal of As to leave In droplets. The surface morphologies are invariably rougher for GaSb, InSb, and InAs using CCl_2F_2/O_2 RIE than for C_2H_6/H_2 RIE, and there is a significant amount of Cl-containing residue on all three materials when using the Freon-12 oxygen chemistry.

Manuscript submitted Oct. 5, 1989; revised manuscript received Jan. 1, 1990.

AT&T Bell Laboratories assisted in meeting the publication costs of this article.

REFERENCES

1. J. M. Woodall, J. L. Freeouf, G. D. Pettit, T. N. Jackson, and P. Kirchner, *J. Vac. Sci. Technol.*, **19,** 626 (1981).
2. S. L. Wright, R. F. Marks, S. Tiwari, T. N. Jackson, and H. Baratte, *Appl. Phys. Lett.*, **49,** 1545 (1986).
3. R. A. Laudise, *J. Cryst. Growth*, **65,** 3 (1983).
4. O. Hilderbrand, W. Kuebart, K. W. Bentz, and M. H. Pilkuhn, *IEEE J. Quant. Electron.*, **QE17,** 284 (1981).
5. W. A. Sunder, R. L. Barns, T. Y. Komotani, J. M. Parsey, Jr., and R. A. Laudise, *J. Cryst. Growth*, **78,** 9 (1986).
6. G. C. Osbourn, *IEEE J. Quant. Electron.*, **QE22,** 1677 (1986).
7. E. L. Hu and R. E. Howard, *Appl. Phys. Lett.*, **37,** 1022 (1980).
8. R. A. Barker, T. M. Mayer, and R. H. Burton, *ibid.*, **40,** 503 (1982).
9. R. H. Burton, R. A. Gottscho, and G. Smolinsky, "Dry Etching for Microelectronics," R. A. Powell, Editor, Chap. 3, Elsevier Publishing Co., New York (1984).
10. M. B. Stern and P. F. Liao, *J. Vac. Sci. Technol.*, **B1,** 1053 (1983).
11. L. A. Coldren, *Mat. Res. Soc. Symp. Proc.*, **126,** 237 (1988).
12. L. A. Coldren and J. A. Rentschler, *J. Vac. Sci. Technol.*, **19,** 225 (1981).
13. S. W. Pang, *This Journal*, **133,** 784 (1986).
14. A. Scherer, H. G. Craighead, and E. D. Beebe, *J. Vac. Sci. Technol.*, **B3,** 402 (1985).
15. U. Niggebrugge, M. Klug, and G. Garus, *Inst. Phys. Conf. Ser.*, **79,** 367 (1985).
16. N. Vodjdani and P. Parrens, *J. Vac. Sci. Technol.*, **B5,** 1591 (1987).
17. R. Cheung, S. Thoms, S. P. Beamont, G. Doughty, V. Law, and C. D. W. Wilkinson, *Electron. Lett.*, **23,** 857 (1987).
18. D. Lecrosnier, L. Henry, A. LeCorre, and C. Vaundry, *ibid.*, **23,** 1254 (1987).
19. T. Matsui, H. Sugimoto, T. Ohnishi, and H. Ogata, *ibid.*, **24,** 798 (1988).
20. S. J. Pearton, U. K. Chakrabarti, and W. S. Hobson, *J. Appl. Phys.*, **66,** 2061 (1989).
21. H. Schmid, "Proceedings of the 6th International Conference on Ion and Plasma Assisted Techniques," Brighton, UK, p. 98, Elsevier Publishing Co., New York and Amsterdam (1987).
22. L. Henry and C. Vaudry, *Electron. Lett.*, **23,** 1253 (1987).
23. J. Allegre and M. Averous, *Inst. Phys. Conf. Ser.*, **46,** 379 (1977).
24. K. Nakasima, *Jpn. J. Appl. Phys.*, **20,** 1085 (1981).
25. M. Lee, D. J. Nicholas, K. E. Singer, and B. Hamilton, *J. Appl. Phys.*, **59,** 2895 (1986).
26. A. Brown, J. A. Van den Berg, and J. C. Vickerman, *Surf. Interface Anal.*, **9,** 309 (1986).
27. S. J. Pearton, A. R. Von Neida, J. M. Brown, K. T. Short, L. J. Oster, and U. K. Chakrabarti, *J. Appl. Phys.*, **64,** 629 (1988).
28. "Handbook of Chemistry and Physics," CRC Press, Boca Raton, FL (1985).
29. O. Kubachewski and C. B. Alcock, "Metallurgical Thermochemistry," 5th ed., Pergamon Press, New York (1979).
30. "Comprehensive Inorganic Chemistry," Vol. 1, J. C. Bailer, H. J. Emelus, R. Nyholm, and A. F. Trotman-Dickerson, Editors, Pergamon Press, Ltd., New York (1973).
31. C. W. Tu, R. P. H. Chang, and A. R. Schlier, *Appl. Phys. Lett.*, **41,** 80 (1982).